

CONSTRAINED TRAJECTORY GENERATION FOR MICRO-SATELLITE FORMATION FLYING

Mark B. Milam, Nicolas Petit, and Richard M. Murray
 Control and Dynamical Systems
 Mail Code 107-81
 California Institute of Technology
 Pasadena, CA 91125.
 {milam,npetit,murray}@cds.caltech.edu

ABSTRACT

Station-keeping and reorientation control of a cluster of fully-actuated low-thrust micro-satellites is considered in this paper. We propose a very general optimization based control methodology to solve constrained trajectory generation problems for stationkeeping and reorientation. By taking advantage of the fully-actuated structure of the micro-satellite, it is possible to compute the control on-board the micro-satellites. Performance of this methodology is reported for a typical micro-satellite formation flying space mission using the Nonlinear Trajectory Generation software package.

Keywords: Formation Flying, Coordinated Optimal Control.

1 INTRODUCTION

Several proposed earth orbiting demonstration space missions plan to utilize formations of cooperating fully-actuated micro-satellites to perform the function of a single complex satellite. The Air Force space based radar system called TechSat21¹² is a prime example of such a mission. One of the challenges of these missions is the formation control of the micro-satellites to meet a unified objective. Two typical formation control problems are the following:

1. Station-keeping: A distributed array of small micro-satellite apertures will collaborate to form a much larger aperture than that possible with a single satellite.

2. Reconfiguration and Deconfiguration: Distribution of micro-satellite aperture can be dynamically reconfigured or deconfigured to meet changes in imaging or mission requirements.

Under the classical gravitational potential assumption, a standard approach to the formation control problem is to linearize the dynamics of the satellites around some reference orbit. In the case that the reference orbit is circular with no perturbative forces, the linearized equations of motion are commonly referred to as the Clohessy-Wiltshire equations.¹ When the correct initial conditions are chosen, the relative positions of the micro-satellites are periodic. By positioning the satellites at different phases along these periodic solutions, a sparse aperture can be created for imaging. Ideally, if satellite positioning is acceptable for imaging, no fuel would be used by taking advantage of the natural dynamics of the vehicles.

However, most micro-satellite missions will be subject to various perturbative forces. The second zonal harmonic of the non spherical Earth (J_2) is a dominant perturbation for the orbits under consideration in this paper and cannot be neglected. The J_2 perturbation acts differentially on each satellite and induces secular motion between the micro-satellites in the formation. Sedwick *et al.*¹¹ derived an analytic expression for exact cancellation of differential J_2 for a micro-satellite formation in a polar, circular orbit. The appropriate choice of initial conditions for a micro-satellite can also mitigate the differential effect of J_2 , see Schaub *et al.*,¹⁰ Vadali *et al.*¹³ and Koon *et al.*⁶

Our approach is based on using optimal control to actively control the sparse aperture of the micro-satellites formation. This has the advantage over existing techniques in that geometric formation constraints can be satisfied for arbitrary orbits. Opti-

Work partially supported by AFOSR grant F49620-99-1-0190 and the Institut National de Recherche en Informatique et Automatique (INRIA)

Copyright © 2001 by the American Institute of Aeronautics and Astronautics, Inc. All rights reserved.

2 PROBLEM FORMULATION

mal control has proven relevant in the absence of J_2 . Kumar *et al.*⁷ used optimal control to solve for the relative motion of two satellites in very low Earth orbits. As a result, Kumar kept the satellites constrained to a box accounting for a generic differential drag perturbation. Inalhan *et al.*⁵ considered the micro-satellite reconfiguration as a distributed and hierarchical control problem. In this paper we will explicitly take the J_2 effect into account and consider a centralized optimal control formulation for a micro-satellite formation. The optimal control problem is then solved using the Nonlinear Trajectory Generation (NTG) software package.

Two strategies will be considered. First, the station keeping control of three satellites: minimize fuel subject to some nonlinear communication and imaging trajectory constraint. Second, the reconfiguration control of three micro-satellites: minimize fuel subject to final time formation constraints.

We will address the formation control problem in terms of the absolute reference frame and not the frame relative to the orbit. This is a challenge since numerical computations must be done with a high degree of accuracy. Yet this point of view simplifies the methodology. Optimal trajectories to linearize about may not be simple periodic trajectories as with a circular orbit with no perturbations. Instead, the trajectories would be expressed as a time varying curve creating complicated expressions for the linearized dynamics. Finding the best trajectories for a *formation* of micro-satellites is a difficult task. The numerical implementation of optimal control for such a strategy would also be complex. Another disadvantage of using the linearization is that large reconfiguration maneuvers may be away from the region where a linearization is valid.

This paper is organized as follows. Section 2 presents the formulation of the problem under consideration. Section 3 provides a brief overview of the nonlinear trajectory generation software that will be used in all computations. The structure of the micro-satellites problem that makes real-time trajectory generation possible is also addressed in this section. Section 4 describes the costs and constraints in order to satisfy typical station keeping and reconfiguration requirements.

Numerical results are given in Section 5. Several trade studies are conducted and simulation results are also presented in this section. Finally, extensions to general classes of perturbations and conclusions are given in Section 6.

The motion of each fully-actuated micro-satellite is described in absolute coordinates. Including the J_2 perturbation, the dynamics are described by the following differential equations

$$\begin{aligned}
 m\ddot{x}_i &= -\frac{\mu x_i}{|r_i|^3} \left(1 - J_2 \frac{3}{2} \left(\frac{R_e}{|r_i|} \right)^2 \left(5 \frac{z_i^2}{|r_i|^2} - 1 \right) \right) + u_{x_i}^I \\
 m\ddot{y}_i &= -\frac{\mu y_i}{|r_i|^3} \left(1 - J_2 \frac{3}{2} \left(\frac{R_e}{|r_i|} \right)^2 \left(5 \frac{z_i^2}{|r_i|^2} - 1 \right) \right) + u_{y_i}^I \\
 m\ddot{z}_i &= -\frac{\mu z_i}{|r_i|^3} \left(1 + J_2 \frac{3}{2} \left(\frac{R_e}{|r_i|} \right)^2 \left(3 - 5 \frac{z_i^2}{|r_i|^2} \right) \right) + u_{z_i}^I
 \end{aligned} \tag{1}$$

where x_i , y_i , and z_i are the coordinates of the absolute position of the *ith* micro-satellite $i \in \{1, 2, 3\}$ and $|r_i| = \sqrt{x_i^2 + y_i^2 + z_i^2}$. The gravitational constant is denoted by μ and the second zonal harmonic of the non-spherical earth effect by J_2 . Superscripts I and B denote the inertial and body frame, respectively. Figure 1 depicts the coordinate systems used throughout this paper. Classically, the local coordinate system is chosen so that the X^O axis points up, the Y^O axis is parallel to the velocity vector and the Z^O axis is in the cross range direction. For the inertial coordinate system, the X^I direction is towards the vernal equinox, the Y^I direction is along the equatorial axis and the Z^I points toward the north pole.

The mass of each satellite is denoted by m and is considered constant (100 kg). It is assumed that the moments of inertia are such that ($I_Z > I_X, I_Y$) so that each micro-satellite is gravity gradient stabilized.

It is assumed that the body frame of the satellite is always aligned to the orbit frame as a result of the passive attitude stabilization. Therefore, it is easy to find the transformation from the body frame to the inertial frame by the following

$$\begin{aligned}
 u^I &= T_{IB} u^B = T_{IO} u^B \\
 T_{IO} &= \left[\left(-\frac{q}{\|q\|} \right) \times \left(\frac{p \times q}{\|p \times q\|} \right), \frac{p \times q}{\|p \times q\|}, -\frac{q}{\|q\|} \right]
 \end{aligned}$$

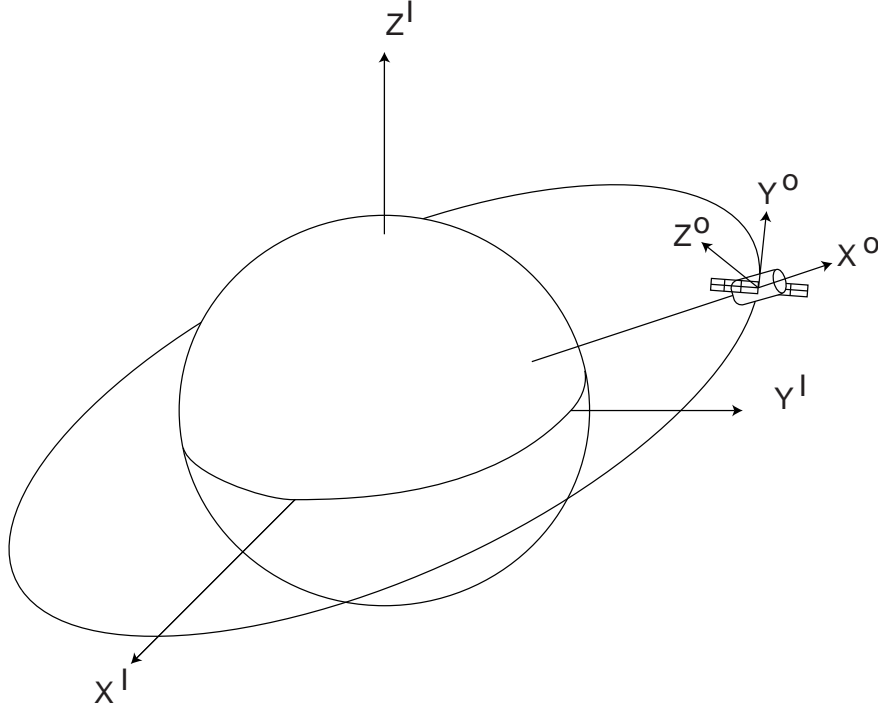


Figure 1: Orbit and inertial coordinate systems.

where $u^I = (u_{x_i}^I, u_{y_i}^I, u_{z_i}^I)^T$, $q = (x, y, z)^T$, $p = (\dot{x}, \dot{y}, \dot{z})^T$. T_{IO} is the transformation from the frame fixed to the orbit to the inertial frame and T_{IB} is the transformation from the body frame to the inertial frame. T_{IB} is a rotation matrix, so $\|u_i^B\| = \|u_i^I\|$ where $\|\cdot\|$ is the Euclidean norm. This particular point will be useful in the optimal problems formulations.

All numerical calculations presented in this paper assume a semi-major axis (a) of 7138 km, which corresponds to an altitude of 800 km for a circular orbit. Eccentricities (e) between 0 and 0.1 are addressed. Generally, the technique presented here can be used for any desired orbit.

3 TRAJECTORY GENERATION METHODOLOGY

To solve the proposed optimal control problems, we use a software package developed at Caltech called NTG. NTG requires a nonlinear programming solver; we will use the sequential quadratic programming package NPSOL by Gill *et al.*⁴ for all numerical calculations in this paper.

There are three primary components to the NTG methodology. The first is to determine outputs such that Equation (1) can be mapped to a lower di-

mensional output space. Once this is done the cost and the constraints can also be mapped to the output space. The second is to parameterize the outputs in terms of B-spline curves. Finally, sequential quadratic programming is used to solve for the coefficients of the B-splines to minimize the cost subject to constraints in output space. This approach has proven relevant in many practical examples and benchmark problems. The reduction of the dimensionality induced by this efficient parameterization allows substantial reduction of the execution time required for solving the nonlinear programming problem. From a practical point of view, this feature allows us to consider real-time applications. See Milam *et al.*⁸ and Petit *et al.*⁹ for complete details on NTG.

The problem of finding a parameterization for this system is particularly easy to solve since, as with any fully actuated mechanical system, each micro-satellite is *flat*, see Fliess *et al.*²³ Namely, by choosing the configuration variables x_i , y_i and z_i , we can parameterize the complete state and inputs x_i , \dot{x}_i , y_i , \dot{y}_i , z_i , \dot{z}_i , $u_{x_i}^I$, and $u_{y_i}^I$ and $u_{z_i}^I$, respectively, this gives $u^B = T_{OI}u^I$ where $T_{OI} = T_{IO}^T$.

Numerical implementation In NTG, a time scaling is required to make the evaluation of the B-spline polynomials accurate. In order not to interfere with the absolute precision of the software package, a time scale was also applied. It turned out that the following scalings worked particularly well for our problem

$$t_s = \frac{t}{S_t}, \quad q_s = \frac{q}{R_e}, \quad m_s = \frac{m}{S_m}.$$

The time was scaled by S_t so that an orbit was approximately one time unit. The inertial positions q were scaled by the radius of the earth R_e and the mass m was scaled by S_m to unity.

4 OPTIMAL CONTROL PROBLEM

Parameterizing the trajectory of the micro-satellites over large periods of time would require prohibitively many variables, rendering real-time computation impossible. Therefore, in order to make the real-time computation tractable, we solve optimal control problems over a finite horizon $[0, T]$. We take T equal to the approximate period of the orbit (without control) and thus solve the optimal control problem for one orbit. Then we take the ending point of this optimal trajectory as a new starting point and solve the optimal control problem over the horizon $[T, 2T]$, *etc.* This methodology, though sub-optimal when compared to the optimal control solution over the whole mission, is numerically tractable and very efficient. Furthermore, it may be necessary to adopt such a strategy to handle unmodeled dynamics and perturbations. All the results given in Section 5 were obtained by this method.

4.1 Station-keeping with guaranteed earth coverage

The instantaneous fuel consumption of each micro-satellite can be represented as $|u_{x_i}^B| + |u_{y_i}^B| + |u_{z_i}^B|$. This non-differentiable function would make our numerical solver behave poorly. To overcome any trouble with the evaluation of the gradient of the cost, we substitute to this cost a classical quadratic cost $(u_{x_i}^B)^2 + (u_{y_i}^B)^2 + (u_{z_i}^B)^2$. Though this does affect the formulation of the optimal control, the solution obtained provides a very low $|u_{x_i}^B| + |u_{y_i}^B| + |u_{z_i}^B|$ cost. Moreover, the mapping from u^B to u^I is such that $\|u^B\| = \|u^I\|$ (see Section 2), which is very convenient for numerical resolution.

Let $T > 0$ be the finite horizon over which we want to solve the optimal control problem. The positions of the three micro-satellites will be denoted by $q_1 = (x_1, y_1, z_1)$, $q_2 = (x_2, y_2, z_2)$, $q_3 = (x_3, y_3, z_3)$

and the thrusts by $u_1^B = T_{OI}(u_{x_1}^I, u_{y_1}^I, u_{z_1}^I)$, $u_2^B = T_{OI}(u_{x_2}^I, u_{y_2}^I, u_{z_2}^I)$, $u_3^B = T_{OI}(u_{x_3}^I, u_{y_3}^I, u_{z_3}^I)$.

We will now cast the requirements for imaging and communications into nonlinear constraints. Determining these constraints are likely to be mission specific. The constraints chosen are purely for illustration to show that complicated nonlinear constraints can be handled with our methodology.

The first constraint we will consider can be written as

$$\|q_i(t) - q_j(t)\| \leq d, \quad \forall t \in [0, T], \forall (i, j) \in \{1, 2, 3\}, i \neq j. \quad (2)$$

We will interpret this as a communication constraints, that is, we desire the micro-satellites to stay close together so that communication between the micro-satellites is possible.

The second constraint we will consider is an imaging constraint. We will require that the area projected on the earth be above some threshold. For sake of simplicity and computational efficiency, we chose not to compute the exact surface of the projection of the triangle defined by the three micro-satellites on the earth. Instead we computed the projection on the earth as if the earth was locally a plane, which is a relevant approximation for areas as small as 1000m².

This ‘‘projected’’ area is, up to an arbitrary choice of orientation

$$A(t) = \frac{1}{2}n(t) \cdot m(t)$$

where

$$\begin{aligned} m(t) &= (q_1(t) + q_2(t) + q_3(t)) / \|q_1(t) + q_2(t) + q_3(t)\| \\ n(t) &= (q_1(t) - q_3(t)) \times (q_1(t) - q_2(t)) \\ &\quad / \|(q_1(t) - q_3(t)) \times (q_1(t) - q_2(t))\|. \end{aligned}$$

The projected area is depicted in Figure 2. The imaging constraint is

$$A(t) \geq S, \quad \forall t \in [0, T]. \quad (3)$$

Finally, we solve the following optimal control problem.

Problem 1 (Station-keeping) Given initial values for the positions and velocities of the three micro-satellites $q_1, q_2, q_3, p_1, p_2, p_3$, we look for a minimum of

$$J(u_1^B, u_2^B, u_3^B) = \int_0^T (\|u_1^B\|^2 + \|u_2^B\|^2 + \|u_3^B\|^2) dt \quad (4)$$

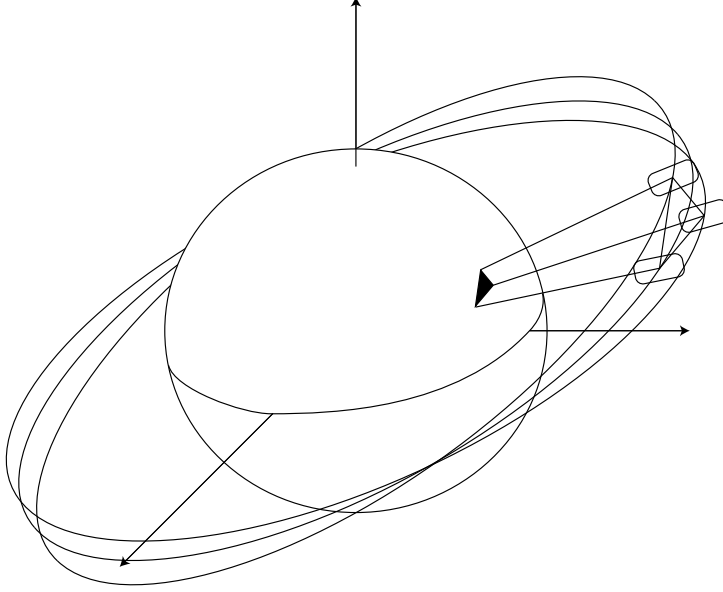


Figure 2: Station keeping with guaranteed earth coverage

subject to the dynamics (1) and the constraints (2), (3).

4.2 Formation reconfiguration and deconfiguration

Given any initial position and velocity of each micro-satellite, we require the three micro-satellites to change their positions and velocities so that the following constraints are satisfied after two orbits:

- the relative distances of the three micro-satellites must be less or equal to a prescribed value
- the projected area on the earth must be no less than a certain value.

These requirements give the following optimal control problem.

Problem 2 (Reconfiguration) Given initial values for the positions and velocities of the three micro-satellites $q_1, q_2, q_3, p_1, p_2, p_3$, we look for a minimum of

$$J(u_1^B, u_2^B, u_3^B) = \int_0^T (\|u_1^B\|^2 + \|u_2^B\|^2 + \|u_3^B\|^2) dt \quad (5)$$

subject to the dynamics (1) and the constraints

$$\begin{aligned} \|q_i(T) - q_j(T)\| &\leq d_f \\ A(T) &\geq a_f. \end{aligned}$$

Moreover, we also solve the inverse problem. Starting from a given triangular configuration, we can compute the thrusts required to go to any prescribed positions and velocities. This can be very useful when imaging of the earth is not necessary. We can ask the micro-satellite to go and wait in a “parking” orbit where they do not burn any fuel. For example, if the satellites were to follow one another on the same free orbit they would not burn fuel or pull apart under J_2 perturbations. When imaging of the earth is necessary, we can reconfigure the micro-satellites into a triangular formation facing the earth and either drift or station keep the formation. These requirements provide the final optimal control problem.

Problem 3 (Deconfiguration) Given initial and final values for the positions and velocities of the three micro-satellites $q_1, q_2, q_3, p_1, p_2, p_3$, we look for a minimum of

$$J(u_1^B, u_2^B, u_3^B) = \int_0^T (\|u_1^B\|^2 + \|u_2^B\|^2 + \|u_3^B\|^2) dt \quad (6)$$

subject to the dynamics (1).

5 NUMERICAL RESULTS

The parameterization of the variables of the system mentioned in section 3 was achieved by using for

each output 10 polynomials or order 9, with 4 regularity conditions at each knot point. This makes a total of 486 coefficients. 70 breakpoints were used to enforce the constraints and evaluate the cost. Orbits without control were used as initial guesses.

The runs were done on several platforms including a Sun computer, a PC using Linux (Red hat 6.2) and a PC running Windows 2000. For the station-keeping problem within one orbit, runs take about 120 seconds, while reconfiguration problems within one orbit take approximately 5 seconds to run. The orbits are approximately 6000 sec. The large difference in computation times is due to the fact that we are enforcing difficult nonlinear trajectory constraints for the station-keeping problem and only a nonlinear final time constraint for the reorientation problem.

5.1 Results to problem 1: Station-keeping under constraints

Let S denote the desired projected surface area and d the maximum distance between allowed between the micro-satellites.

Results for the projected surface area $S = 100 \text{ m}^2$, and the distance between the satellites $d = 500 \text{ m}$ are reported in Figure 3 and Figure 4. Figure 5 depicts the difference in projected area with and without control.

Initial conditions were chosen by perturbing nominal values of orbital elements. The idea being that up to first order the formation should not pull apart if the eccentricity and semi-major axis are chosen the same for all micro-satellites. For instance, we chose $a = 7138 \text{ km}$, $e = 0.1$, $i = 45 \text{ deg}$, $w = 2 \text{ rad}$, $\Omega = 0.1 \text{ rad}$, $M = 0.1 \text{ rad}$ where a is the semi-major axis, e the eccentricity, i the inclination, w argument of periapsis, Ω the longitude of the ascending node, and M the mean anomaly, respectively. And then perturbed this nominal set by $\Delta_1 = (0 \text{ km}, 0, 0 \text{ deg}, -1e - 3 \text{ deg}, 3.5e - 4 \text{ deg}, 0 \text{ deg})$, $\Delta_2 = (0 \text{ km}, 0, 0 \text{ deg}, 5e - 4 \text{ deg}, 0 \text{ deg}, 0 \text{ deg})$ and $\Delta_3 = (0 \text{ km}, 0, 0 \text{ deg}, -1e - 3 \text{ deg}, -3.5e - 4 \text{ deg}, 0 \text{ deg})$ for satellite 1,2 and 3 respectively. There is no particular reason for choosing these initial conditions except that they nominally satisfied the station-keeping constraints.

For this trajectory $i = 45 \text{ deg}$, and the resulting $\Delta V = 10.4 \text{ m/s/year}$. Table 1 contains results of trade studies with eccentricity, inclination, projected surface area S and the maximum distance between satellites d . Many of these results meet a reasonable requirement of a $\Delta V \leq 20 \text{ m/s/year}$. The 90 deg

inclination seems easier to control. While the J_2 effect is more important than in the other cases, the differential J_2 , which really matters, is lower. The controls in the body frame were within $\pm 30 \text{ mN}$ for all cases under consideration.

5.2 Results to problems 2 and 3: Going in and out of triangular formation

We choose to compute optimal reconfiguration within 2 orbits and studied various cases consistent with the station-keeping cases. A typical micro-satellite reconfiguration maneuver is depicted in Figure 6. While the cost of going into a triangular formation decreases with the size of the triangle (constraints are in fact weaker), the cost to come from a triangular formation to a given control-free trajectory increases (the configuration gets harder to recover).

The “parking” strategy seems relevant to useful for mission design. A typical deconfiguration maneuver is depicted in Figure 7. It can be seen in Table 2 that the ΔV cost of a typical “going out of formation” then “going into formation again” is about 0.1 m/s .

The reconfiguration maneuver can be used for a variety of different mission requirements. Reconfiguration of a micro-satellite formation to view a specific region of the earth is one possibility. Another possible using of configuration is to move the formation in a configuration such that it can drift while imaging. When the formation drifts apart, the formation can be reconfigured to drift again.

6 CONCLUSION AND FUTURE WORK

Many perturbations were not taken into account in this work such as solar pressure, aerodynamics drag, etc. Depending on the orbit other perturbations (such as aerodynamic at very low earth orbits) may be dominant. The technique we presented may be generalized to include any perturbation that can be modeled as a function of the positions and their time derivatives since the model remains *flat*.

The choice of initial conditions seems also a critical issue. Using tools from dynamical systems theory, Koon *et al.*⁶ showed that some regions of space offer better initial conditions than others for the station-keeping problem. Starting from these regions of space, we may expect even lower fuel consumptions with the same requirements.

The main result of this work is to report that it is possible to solve problems of engineering interest for micro-satellite formation flying missions by a trajec-

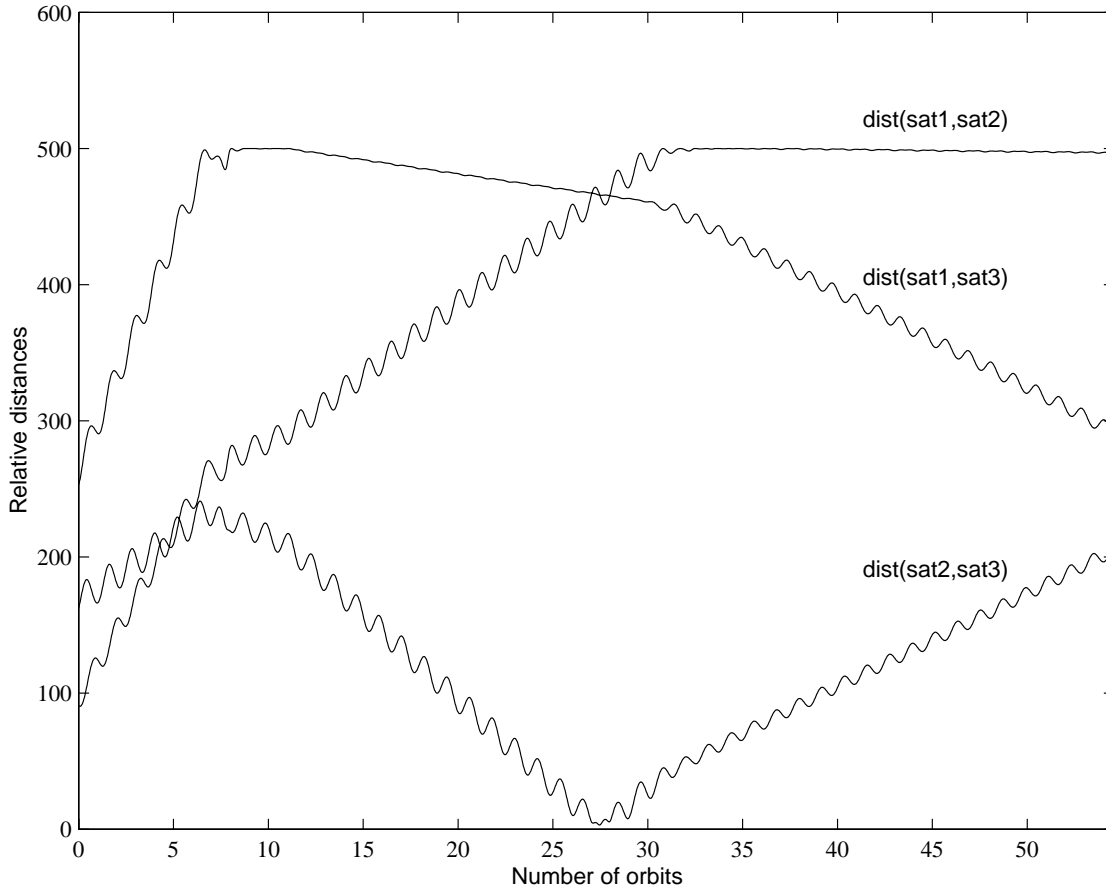


Figure 3: Station-keeping for three micro-satellites. Relative distances (m)

tory generation approach. These trajectories can be computed on board in real-time using NTG.

Acknowledgement Special thanks to Wang Sang Koon for many useful discussions on microsatellite formation flying.

REFERENCES

- [1] W. Clohessy and R. Wiltshire. Terminal guidance system for satellite rendezvous. *Journal of Aerospace Sciences*, 27(9):653–658, 1960.
- [2] M. Fliess, J. Lévine, P. Martin, and P. Rouchon. Flatness and defect of non-linear systems: introductory theory and examples. *International Journal of Control*, 61(6):1327–1360, 1995.
- [3] M. Fliess, J. Lévine, P. Martin, and P. Rouchon. A Lie-Bäcklund approach to equivalence and flatness of nonlinear systems. *IEEE Trans. Auto. Cont.*, 44(5):928–937, 1999.
- [4] P. Gill, W. Murray, M. Saunders, and M. Wright. *User's Guide for NPSOL 5.0: A Fortran Package for Nonlinear Programming*. Systems Optimization Laboratory, Stanford University, Stanford, CA 94305.
- [5] G. Inalhan, J. Busse, and J. How. Precise formation flying control of multiple spacecraft using carrier-phase differential GPS. In *Proc. Guidance, Control and Navigation Conference*, number AAS 00-109, 2000.
- [6] W. S. Koon, J. E. Marsden, J. Masdemont, and R. M. Murray. J_2 dynamics and formation flight. In *Proceedings of AIAA Guidance, Navigation, and Control Conference, Montreal, Quebec, Canada*, 2001.
- [7] R. Kumar and H. Seywald. Fuel-optimal stationkeeping via differential inclusions. *Jour-*

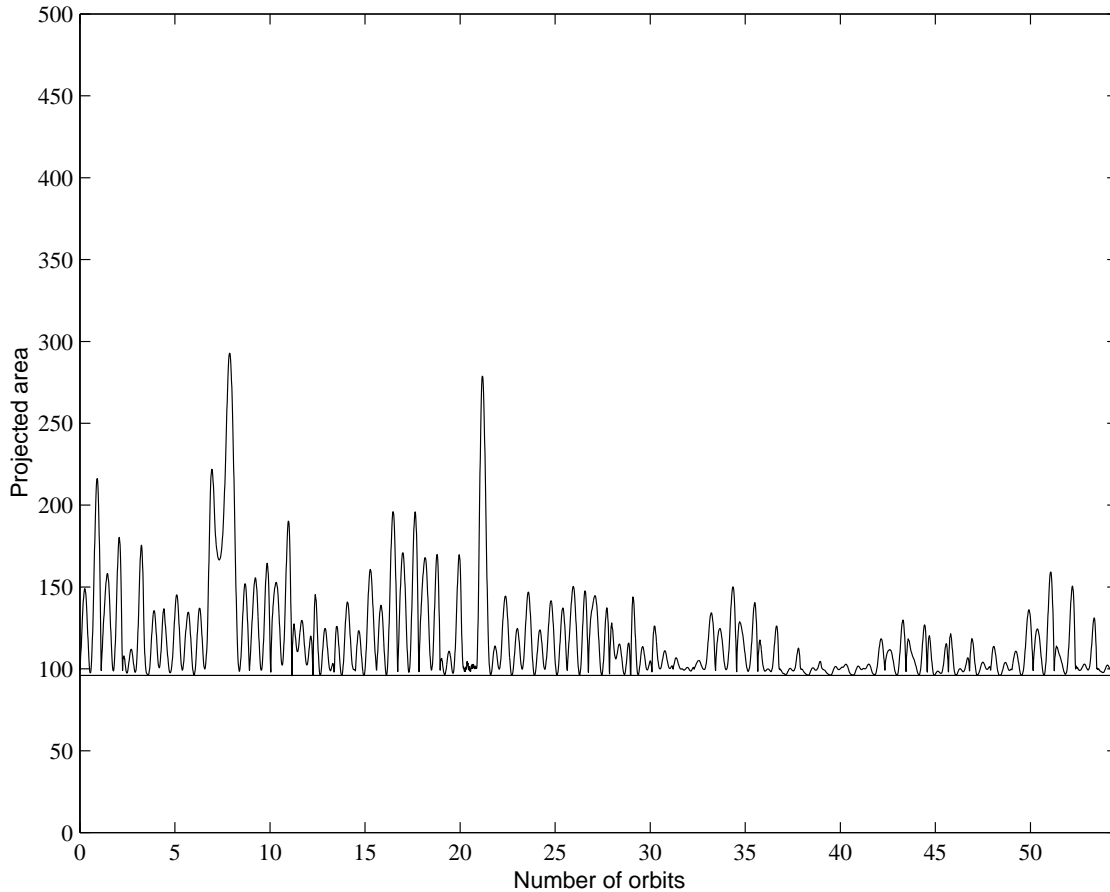


Figure 4: Station-keeping for three micro-satellites. Projected area (m^2).

- nal of Guidance, Control, and Dynamics*, 18(5):1156–1162, 1995.
- [8] M. B. Milam, K. Mushambi, and R. M. Murray. A new computational approach to real-time trajectory generation for constrained mechanical systems. In *IEEE Conference on Decision and Control*, 2000.
- [9] N. Petit, M. B. Milam, and R. M. Murray. Inversion based constrained trajectory optimization. In *5th IFAC symposium on nonlinear control systems*, 2001.
- [10] H. Schaub and K. Alfriend. J_2 invariant relative orbits for spacecraft formation. In *NASA GSFC Flight Mechanics and Estimation Conference*, May 1999.
- [11] Y. Sedwick, D. Miller, and E. Kong. Mitigation of differential perturbations in formation flying satellite clusters. *Journal of Astronautical Sciences*, 47(3 and 4):309–331, 1999.
- [12] TechSat 21. <http://www.vs.afrl.af.mil/vsd/techsat21/> .
- [13] S. Vadali, H. Schauband, and K. Alfriend. Initial conditions and fuel-optimal control for formation flying of satellites. In *AIAA Guidance, Navigation and Control Conference*, August 1999.

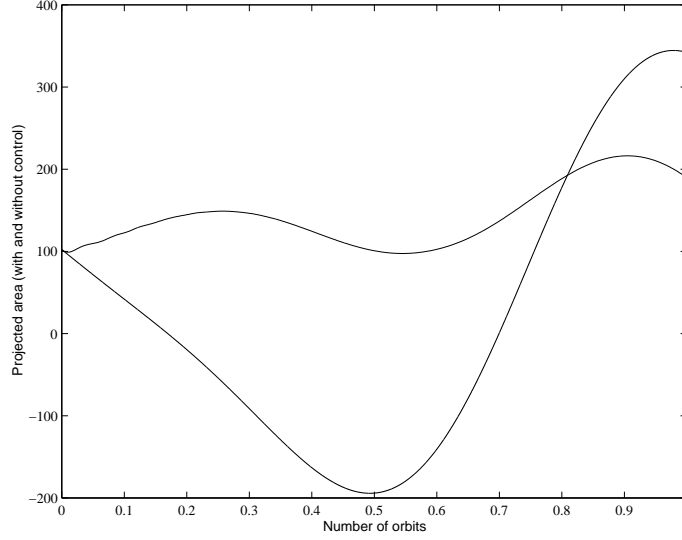


Figure 5: Projected area for stationkeeping with and without control. Projected area (m^2). Without control the projected area becomes singular.

Table 1: Station-keeping. Top: effect of S for a given d . Bottom: effect of e for a given S .

$i = 0 \text{ deg}$	$S = 100 \text{ m}^2$	$S = 200 \text{ m}^2$	$S = 300 \text{ m}^2$
$d \leq 500 \text{ m}$	$\Delta V = 25.6 \text{ m/s/year}$	$\Delta V = 47.8 \text{ m/s/year}$	$\Delta V = 67.3 \text{ m/s/year}$
$i = 45 \text{ deg}$	$S = 100 \text{ m}^2$	$S = 200 \text{ m}^2$	$S = 300 \text{ m}^2$
$d \leq 500 \text{ m}$	$\Delta V = 10.4 \text{ m/s/year}$	$\Delta V = 17.0 \text{ m/s/year}$	$\Delta V = 26.8 \text{ m/s/year}$
$i = 90 \text{ deg}$	$S = 100 \text{ m}^2$	$S = 200 \text{ m}^2$	$S = 300 \text{ m}^2$
$d \leq 500 \text{ m}$	$\Delta V = 8.69 \text{ m/s/year}$	$\Delta V = 21.4 \text{ m/s/year}$	$\Delta V = 27.4 \text{ m/s/year}$

$i = 0 \text{ deg}$	$e = 0$	$e = 0.1$
$S \geq 100 \text{ m}^2, d \leq 500 \text{ m}$	$\Delta V = 25.6 \text{ m/s/year}$	$\Delta V = 36.7 \text{ m/s/year}$
$S \geq 100 \text{ m}^2, d \leq 300 \text{ m}$	$\Delta V = 34.2 \text{ m/s/year}$	$\Delta V = 33.2 \text{ m/s/year}$
$i = 45 \text{ deg}$	$e = 0$	$e = 0.1$
$S \geq 100 \text{ m}^2, d \leq 500 \text{ m}$	$\Delta V = 10.4 \text{ m/s/year}$	$\Delta V = 26.0 \text{ m/s/year}$
$S \geq 100 \text{ m}^2, d \leq 300 \text{ m}$	$\Delta V = 37.0 \text{ m/s/year}$	$\Delta V = 34.2 \text{ m/s/year}$
$i = 90 \text{ deg}$	$e = 0$	$e = 0.1$
$S \geq 100 \text{ m}^2, d \leq 500 \text{ m}$	$\Delta V = 8.69 \text{ m/s/year}$	$\Delta V = 26.1 \text{ m/s/year}$
$S \geq 100 \text{ m}^2, d \leq 300 \text{ m}$	$\Delta V = 21.7 \text{ m/s/year}$	$\Delta V = 28.9 \text{ m/s/year}$

Table 2: Reconfiguration ΔV for various objectives.

Projected area objective (m^2)	150	200	300	400	500	600
Bound on relative distances (m)	150	200	300	400	500	600
Going in formation $\Delta V(\text{m/s})$	1.49e-1	1.09e-1	7.04e-2	4.25e-2	1.20e-2	9.44e-3
Going out of formation $\Delta V (\text{m/s})$	1.23e-2	1.02e-2	1.32e-2	2.62e-2	3.07e-2	4.89e-2

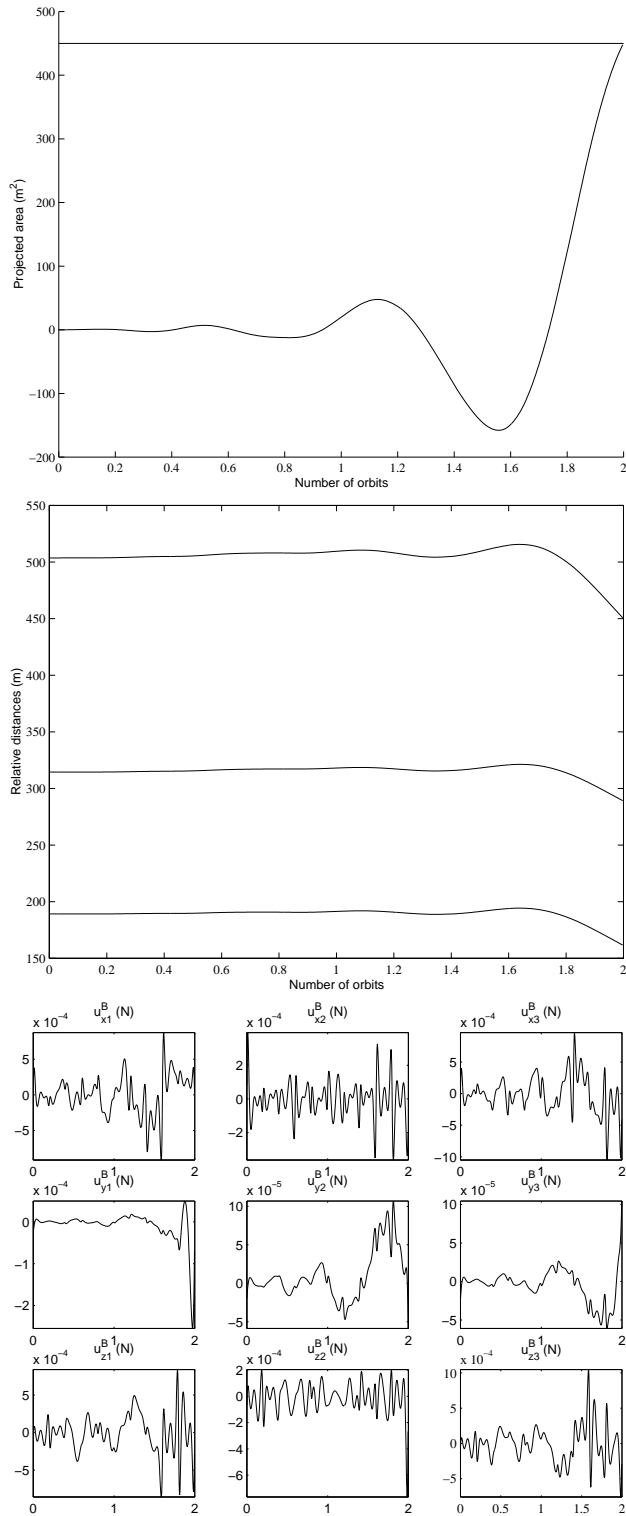


Figure 6: Reconfiguration. Going to a formation with a projected area of $450m^2$. Top: projected area versus time. Middle: relative distances versus time. Bottom: thrusts in the body frame.

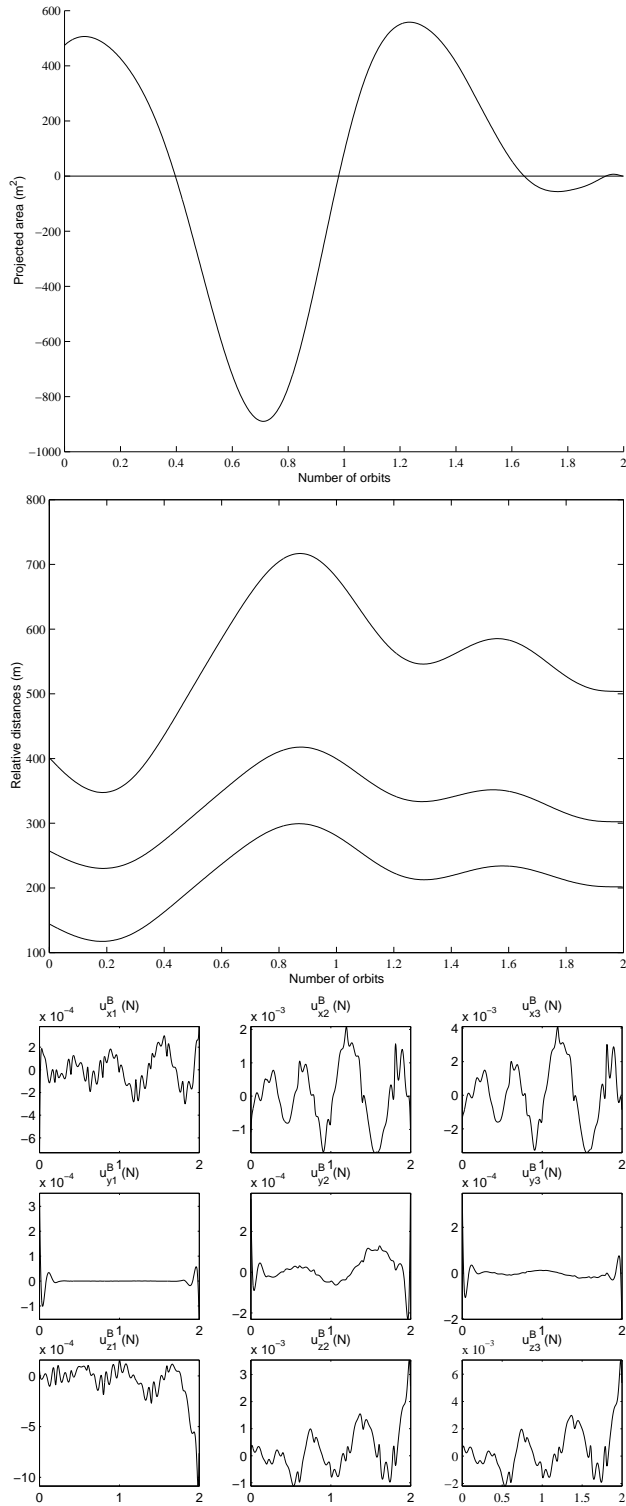


Figure 7: Deconfiguration. Going to a “parking” configuration. Top: projected area versus time. Middle: relative distances versus time. Bottom: thrusts in the body frame.